Available online at www.sciencedirect.com
ScienceDirect
Catalysis Today 116 (2006) 461–468
CATALYSIS TODAY
www.elsevier.com/locate/cattod

Hydrodesulfurization of dibenzothiophene over exfoliated MoS_2 catalyst

Ching Thian Tye, Kevin J. Smith *

Department of Chemical and Biological Engineering, University of British Columbia, 2360 East Mall, Vancouver, BC V6T 1Z3, Canada

Available online 25 July 2006

Abstract

The activity of exfoliated MoS_2 in hydrodesulfurization of dibenzothiophene (DBT) was compared to crystalline MoS_2, molybdenum naphthenate (MoNaph) derived MoS_2 and ammonium heptamolybdate (AHM) derived MoS_2. The prepared catalysts had significantly different morphologies, as described by the crystallite stack height and slab length, measured by both XRD and TEM. These data were used to estimate the fraction of rim and edge sites in the crystallites. The DBT turnover frequency (TOF) was highest on the exfoliated MoS_2, whereas the selectivity for hydrogenolysis and hydrogenation reactions was shown to correlate with the fraction of rim or edge sites. Selectivity for hydrogenolysis increased as the fraction of edge sites increased.

Keywords: Exfoliation; Hydrodesulfurization; Structure–activity; Dibenzothiophene

1. Introduction

Hydrodesulfurization (HDS), an important process in the oil refining industry, is the focus of worldwide research because of increasing use of heavy crude oils with high sulfur content and because of global reductions in the allowable sulfur content of automotive fuels [1]. Commercial HDS processes use MoS_2 catalysts, most often supported on Al_2O_3 and promoted with Co or Ni. Unsupported MoS_2 has been used as a model catalyst in studies of HDS reactions [2–7], eliminating support or promoter effects [2,6–8]. Unsupported MoS_2 is also used as a catalyst to transfer hydrogen in heavy oil hydrocracking slurry processes [9].

Understanding the relationship between active sites and the structure of MoS_2 catalysts is important when trying to improve catalyst performance and a number of studies have reported on structure–activity relationships for MoS_2 catalysts [10–12]. Two types of active sites have been identified; one that promotes hydrogenation reactions and a second that promotes hydrogenolysis of the carbon–heteroatom bond of heterocyclic organic compounds present in the oil. Acidic sites are normally associated with the catalyst support.

The activity of MoS_2 is closely related to the edge planes of MoS_2. The active sites are generally accepted to be metallic sites with sulfur vacancies, whereas the basal plane normally with completely coordinated sulfur atoms, is inert [13]. Eijsbouts et al. [14] have shown a clear correlation between HDS conversion and the number of Mo atoms at the corners and edges of MoS_2 crystallites, reported as the MoS_2 dispersion. High-activity commercial catalysts are found to have very high MoS_2 dispersions. The relationship between MoS_2 structure and active sites for hydrogenolysis and hydrogenation during HDS has also been the subject of numerous studies, e.g. Massoth et al. [15,16] concluded that the edge sites of MoS_2 supported on Al_2O_3 are active for hydrogenation, whereas only the corner sites were active for HDS. Based on a geometric model of unsupported MoS_2, Kasztelan et al. [17] claimed that both hydrogenolysis and hydrogenation reactions were catalyzed on all edge planes. Using unsupported MoS_2 crystallites, prepared with a different number of MoS_2 layers, Daage and Chianelli [2] proposed a rim–edge model in which hydrogenation of dibenzothiophene (DBT) to tetrahydrodibenzothiophene (THDBT) occurred exclusively on the top and bottom edge planes (rim sites) while the hydrogenolysis of DBT to biphenyl (BP) was catalyzed on the edge planes. Iwata et al. [7,8] reported that basal planes with

* Corresponding author. Tel.: +1 604 822 3601; fax: +1 604 822 6003.
E-mail address: kjs@interchange.ubc.ca (K.J. Smith).

0920-5861/$ – see front matter © 2006 Elsevier B.V. All rights reserved.
doi:10.1016/j.cattod.2006.06.028

curvature were catalytically active. The hydrogenation active sites of the MoS_2 particles were related to the 'inflection' of the basal plane of the crystalline MoS_2 microdomains. On the other hand, Hensen et al. [10] concluded that the effect of the number of MoS_2 layers on selectivity depended on the reactant molecular size. Increasing MoS_2 layer stacking increased the hydrogenation reaction as well as hydrogenolysis in the HDS of DBT, whereas hydrogenolysis in HDS of thiophene was not a strong function of the number of MoS_2 layers. Recently, Farag et al. [6] investigated the activity of a series of bulk MoS_2 catalysts synthesized from various precursors, using HDS of DBT as a model reaction. An interesting relationship was found between the average number of MoS_2 stacked layers and the HDS selectivity. The HDS selectivity (ratio of the rate constant for direct desulfurization to the rate constant for hydrogenation) passed through a minimum at a crystallite size of 4 nm and then increased with crystallites larger than 5 nm, irrespective of the starting precursor.

Bulk MoS_2 can be exfoliated into single layer platelets held in suspension as reported by Joensen et al. [18]. The unique structure of exfoliated MoS_2 offers an opportunity to investigate the relationship between catalyst structure and activity. Unsupported exfoliated MoS_2 was reported to have better thiophene HDS conversion compared to unsupported MoS_2 before exfoliation [19,20]. However, an attempt by Del Valle et al. [21] to compare the catalyst activities in HDS of DBT was not successful. Lower activities were reported in cases using exfoliated MoS_2 catalysts. Del Valle et al. [21] suggested that the exfoliated catalysts were poisoned by the lithium used in the exfoliation process.

In the present study the activity of unsupported, exfoliated MoS_2 catalyst is compared with crystalline MoS_2 and MoS_2 catalysts prepared by in situ thermal decomposition of catalyst precursors, yielding vastly different structures of MoS_2. The activity and selectivity of these materials has been investigated using DBT as a model reactant. DBT allows one to study catalyst selectivity for hydrogenolysis and hydrogenation reactions.

2. Experimental

2.1. Catalyst preparation

Four different MoS_2 catalysts were studied in the present work. Two catalysts were prepared by in situ decomposition of soluble Mo precursors—molybdenum naphthenate (MoNaph) from ICN Biomedicals Inc. and ammonium heptamolybdate tetrahydrate, $(NH_4)_6Mo_7O_{24}{\cdot}4H_2O$ (AHM) from Sigma–Aldrich. The third catalyst was commercially available crystalline MoS_2 powder (99%) from Sigma–Aldrich, used without further treatment and the fourth catalyst was the laboratory prepared exfoliated MoS_2.

Exfoliation was carried out under argon atmosphere in a glove box using a slightly modified method of Joensen et al. [18]. MoS_2 powder was soaked in hexane containing *n*-butyllithium (Li:Mo ratio = 1). The suspension was sealed in a sample bottle and left to stand for at least 72 h so that all the Li was intercalated into the MoS_2. The intercalated MoS_2 settled to the bottom and the top layer of solution was decanted. The Li-intercalated MoS_2 was subsequently exposed to water and sonicated for 30 min followed by 30 min of stirring. Excess *n*-butyllithium was removed by a series of washing steps in which the exfoliated MoS_2 was separated by centrifuge and re-dispersed in water. The washing process was repeated until the solution pH reached 7. Finally, the washing process was repeated three more times, replacing water with isopropanol and isopropanol with decalin. The exfoliated MoS_2 dispersion was adjusted to 2 wt.% of MoS_2 dispersed in decalin.

2.2. Activity measurement

Reactions were carried out in a 300 ml Autoclave Engineers stirred, batch reactor loaded with 100 ml of *n*-hexadecane, 900 ppm S equivalent dibenzothiophene and 600 ppm Mo equivalent of the MoS_2 catalyst. The reactor was pressurized by H_2(95%)/H_2S(5 %) to 2.8 MPa at room temperature and stirred at 1200 rpm and then heated at a rate of 10 °C/min to 350 °C. The reaction proceeded at this temperature for 5 h. During the reaction, liquid samples (3–5 ml) were withdrawn at 30 min intervals for the first 2 h then at 1 h intervals for the remaining 3 h. After reaction, the solids present in the reactor were recovered by filtration, washed with pentane, vacuum dried for 3 h at 100 °C and dried further at 160 °C for 2 h before characterization.

Liquid samples were analyzed with a Shimadzu gas chromatograph (model GC-14A) fitted with a capillary column (AT-5, 30 m × 0.32 mm × 0.25 μm) and a flame ionization detector. The identities of the products were determined by comparison with pure reference samples and by GC/MS analysis of selected liquid samples.

2.3. Catalyst characterization

Catalyst X-ray diffraction (XRD) patterns were recorded with a Siemens D5000 powder diffractometer operated at 40 kV and 30 mA using Cu Kα radiation (λ = 1.5406 Å). The crystallite size of MoS_2 was determined using the (0 0 2) diffraction peak and the Scherrer equation:

$$H = \frac{0.89\lambda}{\beta \cos 7.2^\circ}$$

Table 1
Properties of different MoS_2 catalysts

Catalyst	BET surface area (m^2/g)	Slab length, L (nm)	Stack height, H (nm)	Number of layers
Crystalline MoS_2	4.2	560	35.8	57
Exfoliated MoS_2	7.8	400	5.5	9
MoNaph derived MoS_2	253	10	1.8 (0.8[a])	2.8 (1.3[a])
AHM derived MoS_2	–	9.3	2.1 (1.1[a])	3.3 (1.8[a])

[a] As determined from TEM micrographs.

where H is the average crystallite size of MoS_2 for the plane perpendicular to the basal plane; λ is the wavelength (Cu Kα) and β is the corrected half-width of the diffraction peak.

BET surface areas were measured by N_2 adsorption at −196 °C using a FlowSorb II 2300 Micromeritics analyzer. Samples were degassed at 150 °C for 2 h prior to measurement. The precision of the measurements was within ±5%. Bulk compositions of the catalysts were estimated using energy dispersive X-ray emission (EDX) with a Hitachi S300N scanning electron microscope operated at 20 kV.

Transmission electron microscopy (TEM) was performed under high-resolution mode on a Hitachi H7600 electron microscope operated at 200 kV. After grinding with pestle and mortar, each catalyst sample was dispersed in ethanol and deposited on a carbon-coated copper grid. The specimen was dried in air prior to analysis. From different representative micrographs, the length of at least 100 MoS_2 fringes was measured. The average slab length (L) was used to calculate the number of edge site Mo atoms, n for a single slab using $L = 3.2(2n - 1)$ Å, based on the assumption that the MoS_2 slab was a perfect hexagon, as presented by Kasztelan et al. [17]. The MoS_2 dispersion, f_{Mo} was calculated by dividing the total amount of Mo at the edge surface by the total number of Mo atoms using the slab size determined from the TEM micrographs [10]. The following equation gives f_{Mo} in terms of n and x, x being the total number of slabs:

$$f_{Mo} = \frac{\sum_{i=1,\ldots,x} 6n_i - 6}{\sum_{i=1,\ldots,x} 3n_i^2 - 3n_i + 1}$$

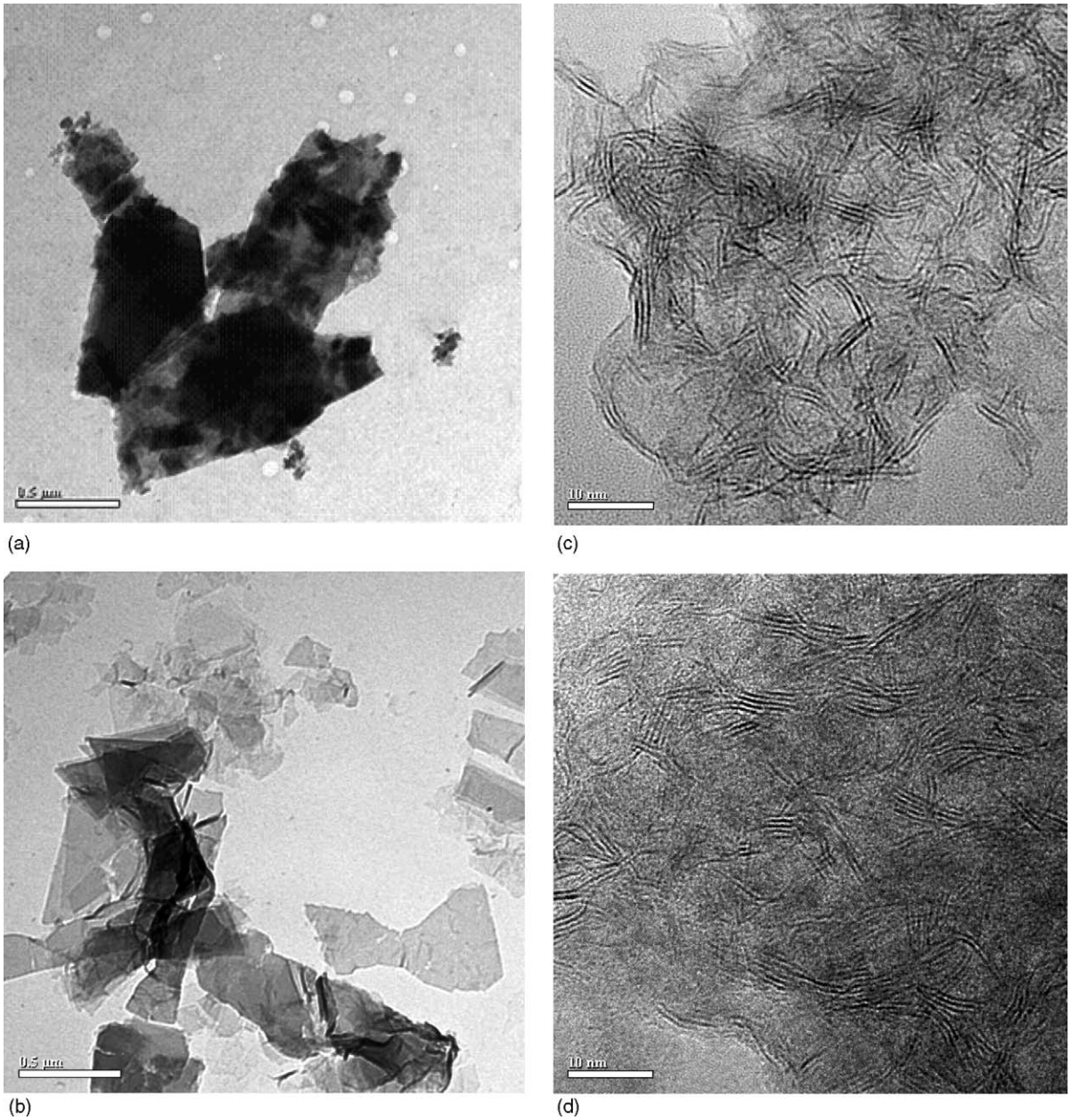

Fig. 1. TEM of: (a) crystalline MoS_2, (b) exfoliated MoS_2, (c) MoNaph derived MoS_2 and (d) AHM derived MoS_2.

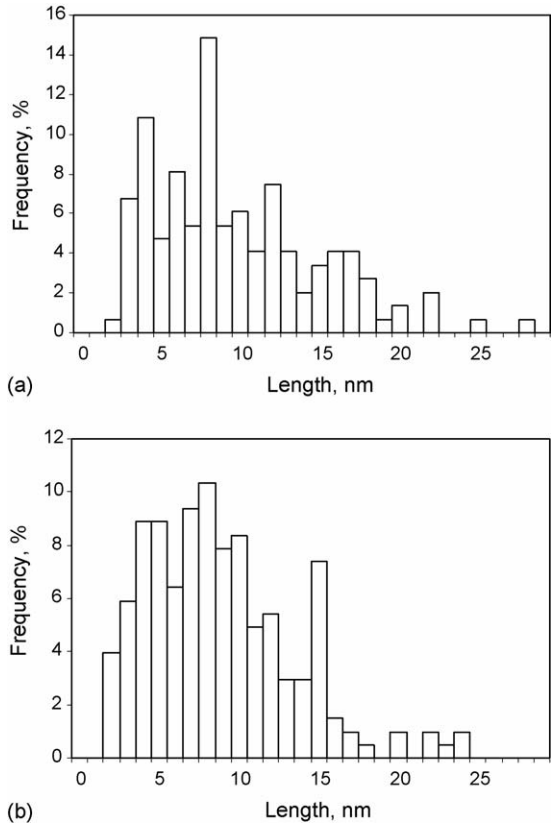

Fig. 2. Distribution of MoS_2 slab length for: (a) MoNaph and (b) AHM derived MoS_2 (from TEM analysis).

3. Results and discussion

3.1. Catalyst characterization

The MoS_2 prepared from MoNaph and AHM was characterized by recovering the solid MoS_2 after reaction. EDX analyses of the recovered solid confirmed the presence of Mo and S alone, with an average S/Mo atom ratio of 2.5 ± 0.2. BET surface area analysis (Table 1) showed that the crystalline

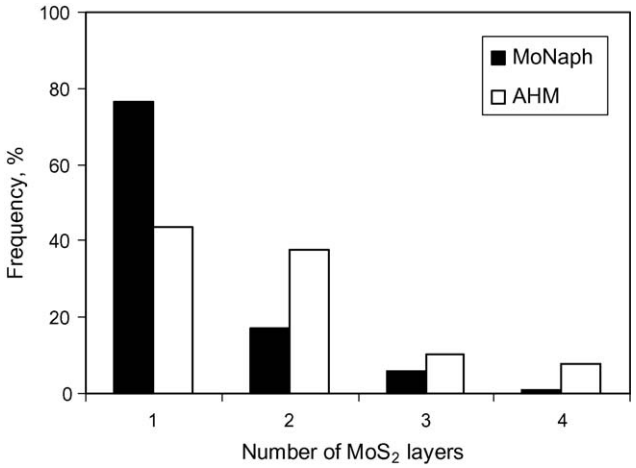

Fig. 3. Distribution of the number of layers for MoNaph and AHM derived MoS_2.

MoS_2 (4.2 m^2/g) and exfoliated MoS_2 (7.8 m^2/g) had comparable areas, whereas MoNaph derived MoS_2 had a significantly higher BET area of 253 m^2/g. The high surface area of the MoNaph derived MoS_2 was likely due to the formation of solid carbon during the decomposition of MoNaph, which also preserved the high dispersion of MoS_2 [22]. The BET area of the AHM derived MoS_2 was not determined since the amount recovered after reaction was insufficient for BET analysis.

The average stack height of the MoS_2 particles, estimated from the XRD line-broadening of the (0 0 2) peak was 35.8, 5.5, 1.8 and 2.1 nm for crystalline MoS_2, exfoliated MoS_2, MoNaph derived MoS_2 and AHM derived MoS_2, respectively. The average number of MoS_2 layers, calculated from the stack height, is shown in Table 1.

TEM micrographs of the four catalysts are shown in Fig. 1(a–d). The slab length of the crystalline MoS_2 and exfoliated MoS_2 was an order of magnitude larger than that of MoNaph and AHM derived MoS_2. MoNaph and AHM derived MoS_2 each exhibited a similar slab length of about 10 nm. The average slab length of these two catalysts, shown in Table 1,

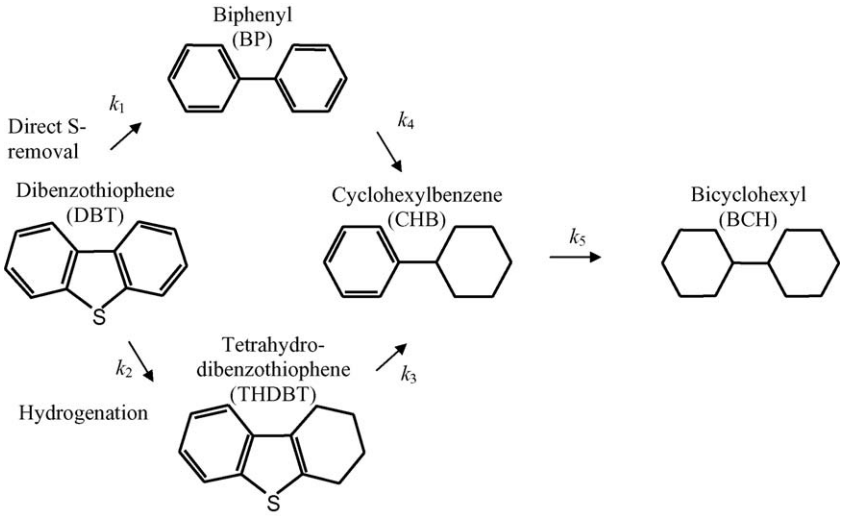

Fig. 4. Reaction network of dibenzothiophene.

Table 2
DBT conversion and HDS conversion for different catalysts after 5 h reaction at 350 °C and 2.8 MPa initial pressure with 600 ppm Mo

Catalyst	DBT conversion (%)	HDS conversion (%)
Crystalline MoS_2	12.6	8.9
Exfoliated MoS_2	35.3	25.8
MoNaph derived MoS_2	15.9	3.3
AHM derived MoS_2	99.2	95.8

was calculated from the distribution of MoS_2 slab lengths (Fig. 2) determined from the TEM micrographs. The distribution of the number of MoS_2 layers for MoNaph and AHM derived MoS_2 were also determined from the TEM micrographs and are shown in Fig. 3. The average number of layers for MoNaph and AHM was 1.3 and 1.8, respectively. This result is lower than that obtained from the line-broadening of (0 0 2) peak in the XRD pattern and confirms that MoNaph and AHM lead to highly dispersed MoS_2.

In summary, four MoS_2 catalysts were prepared each with different morphology. The exfoliated MoS_2 had an average of nine layers of MoS_2 in a large sheet morphology (0.40 μm) compared to the crystalline MoS_2 with 57 layers and average slab length of 0.56 μm. In contrast, MoS_2 derived from MoNaph and AHM precursors had a slab length of approximately 10 nm with one to two layers of MoS_2 in the crystallites.

3.2. Activity of catalysts

The major products of DBT conversion from all the catalysts were tetrahydro-dibenzothiophene (THDBT), biphenyl (BP), cyclohexylbenzene (CHB), and bicyclohexyl (BCH), in agreement with the literature [2,4,5]. BP is a product of direct desulfurization of DBT whereas THDBT is a product of hydrogenation of DBT. CHB could be produced through hydrogenolysis of THDBT or hydrogenation of BP. BCH is a consequent hydrogenation product of CHB. The total yield of desulfurized compounds is defined as the HDS conversion. The HDS reaction network for DBT is depicted in Fig. 4.

Table 2 compares the DBT conversion and HDS conversion of the four different catalysts at 350 °C and an initial pressure of 2.8 MPa. After a 5-h batch reaction, the order of DBT conversion achieved was crystalline MoS_2 (12.6%) < MoNaph derived MoS_2 (15.9%) < exfoliated MoS_2 (35.3%) < AHM derived MoS_2 (99.2%). However, the order in terms of HDS conversion was MoNaph derived MoS_2 (3.3%) < crystalline MoS_2 (8.9%) < exfoliated MoS_2 (25.8%) < AHM derived MoS_2 (95.8%).

Fig. 5 shows the product yields as a function of DBT conversion for each of the four catalysts. Over exfoliated MoS_2 and crystalline MoS_2 the yield of BP was greater than the yield of THDBT for all DBT conversions (Fig. 5(a and b)). Over MoNaph and AHM derived MoS_2, the THDBT yield was greater than the BP yield at the same DBT conversion (below 30%) (Fig. 5(c and d)). Furthermore, at the same DBT conversion, the yield of BP decreased in the order crystalline MoS_2 > exfoliated MoS_2 > MoNaph derived MoS_2 ≈ AHM derived MoS_2. Fig. 5 also shows that all catalysts give a similar profile for the total yield of the final products, CHB and BCH (increasing with increasing DBT conversion). These results demonstrate that the four MoS_2 catalysts have different kinetics of reaction for DBT conversion.

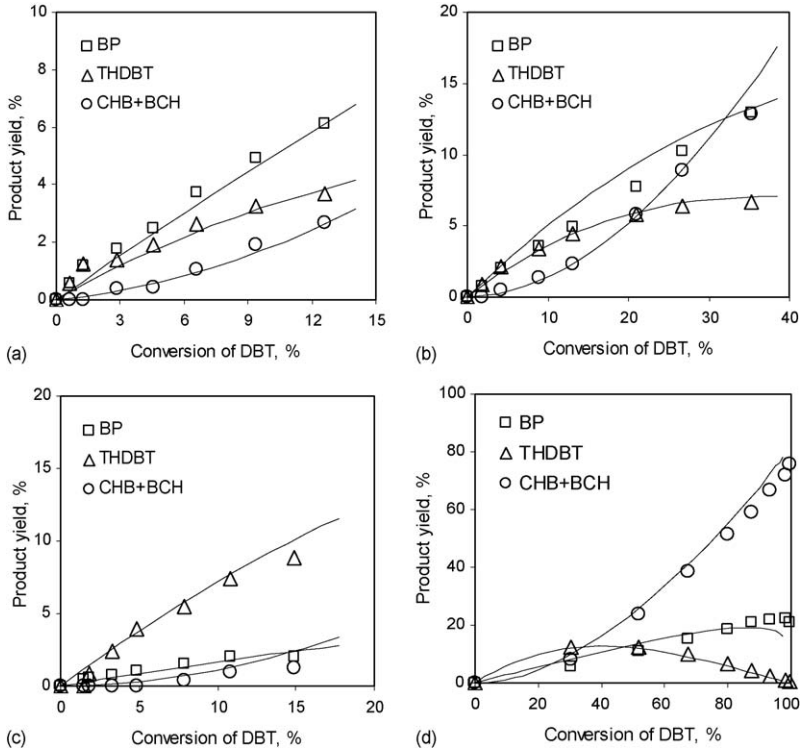

Fig. 5. Products yield vs. conversion of DBT at 350 °C for (a) crystalline MoS_2, (b) exfoliated MoS_2, (c) MoNaph and (d) AHM derived MoS_2 (—fitted model).

Table 3
Dispersion of MoS_2 catalysts

Catalyst	Dispersion, f_{Mo} (%)
Crystalline MoS_2	0.23
Exfoliated MoS_2	0.32
MoNaph derived MoS_2	9.72
AHM derived MoS_2	10.71

To clarify the kinetics of the HDS of DBT, the rate constants of the reaction steps shown in Fig. 4 were estimated for each of the catalysts studied. Each step was assumed to follow first order kinetics and since the amount of hydrogen in the reaction vessel was in excess, the dependency of the reaction kinetics on H_2 pressure can be neglected. The rate constants were estimated using the Gauss–Newton optimization method [23]. Note that although the first order assumption is oversimplified for HDS of DBT, this assumption has been widely used in comparative catalyst studies [6,7] as in the present work. Errors associated with the estimated rate constants were ±10%.

The estimated rate constants were corrected for the amount of Mo at the edge surface of the MoS_2 crystallites using the Mo dispersion, f_{Mo} given in Table 3. The overall reaction rate constants and the initial turnover frequency (TOF), determined for the HDS of DBT over the different catalysts, are summarized in Table 4. The TOF is defined as the number of molecules reacting per active site per unit time and the initial TOF was calculated from the estimated rate constant and the initial concentration of reactant used in the reactor.

Roxlo et al. [13] reported a TOF for DBT conversion of approximately 5×10^{-2} molecules/(molecule Mo s) on both amorphous and crystalline MoS_2 at 350 °C. In the present study the TOFs for HDS of DBT over four different MoS_2 catalysts are of similar magnitude, except for the MoNaph derived MoS_2 catalyst (Table 4). The TOF of the MoNaph derived catalyst was about two orders of magnitude lower than that observed on the other catalysts. Previous studies have shown that MoS_2 derived from MoNaph has a significant amount of carbonaceous material associated with the MoS_2 [22,24]. In one study 11 wt.% of carbon was reportedly present in the MoNaph derived MoS_2 catalyst [25]. In the present study, large amounts of solid were recovered after reaction using MoNaph, compared to the other catalysts with the same Mo feed concentration, suggesting the presence of carbonaceous material. Most likely the low activity (or TOF) of this catalyst was a consequence of limited access to the catalyst active sites because of the carbon associated with the MoS_2. To validate this assertion, MoS_2 prepared from AHM that generated small MoS_2 particles of similar size to that obtained from MoNaph, but without the carbonaceous material, was tested. Consistently, the AHM derived MoS_2 exhibited much higher activity than the MoNaph derived MoS_2 in HDS of DBT (95.8% HDS) and had a TOF of the same order of magnitude as that obtained on the crystalline MoS_2 and exfoliated MoS_2 (Table 4).

The TOF for the disappearance of DBT and k_{DBT} were higher on exfoliated MoS_2 than on crystalline MoS_2 or AHM derived MoS_2. One possible explanation of this trend is the presence of active sites on the basal plane of exfoliated MoS_2 in addition to the edge planes. Iwata et al. [7,8] has suggested that active sites are associated with the 'inflection' of the basal plane that corresponds to rim sites of the crystalline MoS_2 microdomains. TEM of the exfoliated MoS_2 sheets suggested the presence of such inflection which may contribute to the active sites associated with hydrogenation and hydrogenolysis. Activity associated with the basal plane of exfoliated MoS_2 has also been reported in [26,27]. The activity of alumina supported MoS_2 catalysts, prepared by exfoliation, was compared to that of traditionally prepared MoS_2 catalyst, using the HDS of thiophene. Although the number of Mo atoms in the edge plane per gram of MoS_2 catalyst prepared by exfoliation was 10 times lower than that of the standard catalyst, it was reported that similar activity per gram Mo was obtained and hence, these authors suggested that the HDS of thiophene can occur on the basal plane of exfoliated MoS_2 [26,27].

HDS of DBT proceeds through direct desulfurization by hydrogenolysis or through hydrogenation reactions, corresponding to the rate constants k_1 and k_2 in Table 4. For MoS_2 catalysts derived from both MoNaph and AHM precursors, the low values of k_1/k_2 show that DBT conversion was favored by aromatic ring hydrogenation (Fig. 4). The ratio k_1/k_2 for the exfoliated MoS_2 ($k_1/k_2 = 1.28$) and the crystalline MoS_2 ($k_1/k_2 = 1.07$) were of similar magnitude and close to unity, indicating that DBT conversion proceeds through both hydrogenation and hydrogenolysis (k_1 and k_2) in parallel with similar selectivity towards direct desulfurization to BP by hydrogenolysis and hydrogenation to THDBT. These characteristics also explain the higher THDBT yield obtained when using MoNaph and AHM derived MoS_2 and the higher BP yield obtained when using exfoliated MoS_2 and crystalline MoS_2 as

Table 4
Rate constant and initial turn over frequency (TOF) for HDS of DBT over different MoS_2 catalysts at 350 °C

Catalyst	Rate constant (ml/mol Mo_e s) × 10^{-2}[a]								Initial TOF[b]
	k_{DBT}	k_1	k_2	k_3	k_4	k_5	k_1/k_2	k_3/k_2	
Crystalline MoS_2	9.51	5.02	4.69	45.2	7.62	–	1.07	9.64	1.98
Exfoliated MoS_2	21.7	11.5	9.04	80.3	34.3	37.2	1.28	8.88	4.36
MoNaph derived MoS_2	0.29	0.05	0.19	0.50	0.40	–	0.24	2.64	0.06
AHM derived MoS_2	7.91	1.51	3.81	19.6	0.88	2.03	0.40	5.15	1.65

[a] Mo_e refers to the number of Mo atoms available at the edge sites.
[b] Unit of TOF is molecule DBT/(Mo_e s) × 10^2.

catalyst (Fig. 5). Note that the curves of Fig. 5 correspond to the calculated yields using the fitted kinetic parameters.

Exfoliated MoS_2 and crystalline MoS_2 had a higher k_3/k_2 ratio ($k_3/k_2 = 8.88$ and 9.64, respectively) than MoNaph and AHM derived MoS_2 ($k_3/k_2 = 2.64$ and 5.15, respectively). The ratio of k_3/k_2 compares the hydrogenolysis activity for THDBT conversion to CHB and the hydrogenation of DBT to THDBT. The ratios k_1/k_2 and k_3/k_2 show that exfoliated MoS_2 and crystalline MoS_2 had a better hydrogenolysis activity than the MoNaph and AHM derived MoS_2, implying that crystalline MoS_2 has more hydrogenolysis sites than poorly crystalline or amorphous MoS_2. Higher hydrogenolysis activity of crystalline MoS_2 compared to that of AHM derived MoS_2 was also reported by Iwata et al. [7].

There are two important differences in the catalyst structure of crystalline MoS_2 and exfoliated MoS_2, compared to MoNaph and AHM derived MoS_2. First, the two former catalysts have larger slab lengths, corresponding to a large basal plane compared to the latter two catalysts. Secondly, the former catalysts have a higher degree of stacking of MoS_2 layers in the crystallites. Since the basal plane is widely accepted to be inert with few active sites, the difference in selectivity among these catalysts is likely due to the different number of MoS_2 layers in the catalyst particle. In the literature, models have been proposed to account for the effect of structure on active sites by distinguishing between edge, corner and rim sites of the MoS_2 crystallite [2]. Knowing the crystallite dimensions (Table 1) the fraction of rim or edge sites can be calculated using the geometric arguments of Kasztelan et al. [17]. Fig. 6 plots the k_1/k_2 ratio and the k_3/k_2 ratio as a function of the edge or rim sites, for the four catalysts studied herein. Both ratios show an increasing trend with an increase in the fraction of edge sites (or alternatively a decreasing trend with increasing fraction of rim sites). Noting that both rate constant ratios (k_1/k_2 and k_3/k_2) are a measure of hydrogenolysis to hydrogenation reactions occurring on the catalysts, we can conclude, in agreement with the model of Daage and Chianelli [2] that hydrogenation is favored on rim sites. Note that the correlation presented here shows a trend over a wide range of catalyst morphologies, in which both stack height and slab length have been varied.

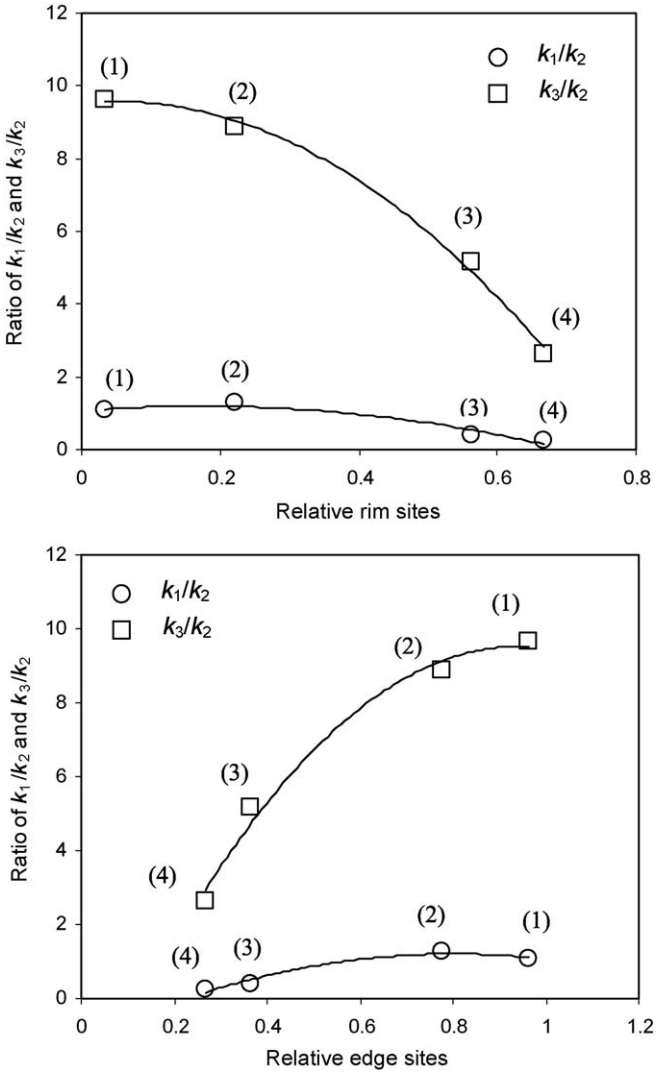

Fig. 6. Ratio of k_1/k_2 and k_3/k_2 vs. relative rim sites and edge sites ((1) crystalline MoS_2; (2) exfoliated MoS_2; (3) AHM and (4) MoNaph derived MoS_2; — trend line).

4. Conclusion

The present study has examined the HDS of DBT over a series of MoS_2 catalysts each with different morphology. The activity of the catalysts towards hydrogenolysis of C–S bonds versus hydrogenation of DBT and THDBT, is shown to correlate with the fraction of edge sites present in the crystallites. Hydrogenolysis selectivity increased as the fraction of edge sites increased, in agreement with the rim–edge model of Daage and Chianelli.

Acknowledgements

Funding from the Natural Sciences and Engineering Research Council of Canada and from Lightyear Inc. is gratefully acknowledged. Tye C.T. acknowledges a fellowship support from Universiti Sains Malaysia and the University of British Columbia.

References

[1] F.L. Plantenga, R.G. Leliveld, Appl. Catal. A 248 (2003) 1.
[2] M. Daage, R.R. Chianelli, J. Catal. 149 (1994) 414.
[3] H. Farag, K. Sakanishi, M. Kouzu, A. Matsumura, Y. Sugimoto, I. Saito, Ind. Eng. Chem. Res. 42 (2003) 306.
[4] M. Del Valle, J. Cruz-Reyes, M. Avalos-Borja, S. Fuentes, Catal. Lett. 54 (1998) 59.
[5] E. Devers, P. Afanasiev, B. Jouguet, M. Vrinat, Catal. Lett. 82 (2002) 13.
[6] H. Farag, K. Sakanishi, M. Kouzu, A. Matsumura, Y. Sugimoto, I. Salto, J. Mol. Catal. A 206 (2003) 399.
[7] Y. Iwata, K. Sato, T. Yoneda, Y. Miki, Y. Sugimoto, A. Nishijima, H. Shimada, Catal. Today 45 (1998) 353.
[8] Y. Iwata, Y. Araki, K. Honna, Y. Miki, K. Sato, H. Shimada, Catal. Today 65 (2001) 335.
[9] A. Del Bianco, N. Panariti, M. Marchionna, Chemtech 25 (1995) 35.
[10] E.J.M. Hensen, P.J. Kooyman, Y. van der Meer, A.M. van der Kraan, V.H.J. de Beer, J.A.R. van Veen, R.A. van Santen, J. Catal. 199 (2001) 224.

[11] H. Schweiger, P. Raybaud, G. Kresse, H. Toulhoat, J. Catal. 207 (2002) 76.
[12] H. Topsoe, B.S. Clausen, Catal. Rev. Sci. Eng. 26 (1984) 395.
[13] C.B. Roxlo, M. Daage, A.F. Ruppert, R.R. Chianelli, J. Catal. 100 (1986) 176.
[14] S. Eijsbouts, J.J.L. Heinerman, H.J.W. Elzerman, Appl. Catal. A 105 (1993) 53.
[15] F.E. Massoth, G. Muralidhar, J. Shabtai, J. Catal. 85 (1984) 53.
[16] W. Zmierczak, G. Muralidhar, F.E. Massoth, J. Catal. 77 (1982) 432.
[17] S. Kasztelan, H. Toulhoat, J. Grimblot, J.P. Bonnelle, Appl. Catal. 13 (1984) 127.
[18] P. Joensen, R.F. Frindt, S.R. Morrison, Mater. Res. Bull. 21 (1986) 457.
[19] M.D. Curtis, Transition metal sulfur chemistry, in: E.I. Steifel, K. Matsumoto (Eds.), ACS Symposium Series 653, American Chemical Society, Washington, DC, (1996), p. 154.
[20] M. Del Valle, M. Avalos-Borja, J. Cruz and S. Fuentes, 351 Mater. Res. Soc. Symp. Proc. Molecularly Designed Ultrafine/Nanostructured Materials, 1994. p. 287.
[21] M. Del Valle, J. Cruz-Reyes, M. Avalos-Borja, S. Fuentes, Catal. Lett. 54 (1998) 59.
[22] N. Rueda, R. Bacaud, M. Vrinat, J. Catal. 169 (1997) 404.
[23] P. Englezos, N. Kalogerakis, Applied Parameter Estimation for Chemical Engineers (Chemical Industries), Marcel Dekker, New York, 2001.
[24] R. Bearden, C.L. Aldrich, Energy Prog. 1 (1981) 44.
[25] N. Rueda, R. Bacaud, P. Lanteri, M. Vrinat, Appl. Catal. A 215 (2001) 81.
[26] D.I. Kochubey, V.P. Babenko, React. Kinet. Catal. Lett. 77 (2002) 237.
[27] D.I. Kochubei, V.A. Rogov, V.P. Babenko, S.V. Bogdanov, V.I. Zaikovskii, Kinet. Catal. 44 (2003) 135.